Aerosol and Air Quality Research

ORIGINAL RESEARCH
https://doi.org/10.4209/aaqr.210382

Reducing the Accumulative Charge on Fabric Filter Surfaces by Using a Bipolar Precharger

Pei Jia*, Manqing Lin*

School of Resources and Safety Engineering, Wuhan Institute of Technology, Wuhan 430073, China

ABSTRACT

This study fabricated a wire-tube bipolar precharger with one power supply to reduce the amount of charge accumulated on fabric filters and improve collection efficiency in a hybrid electrostatic filtration system. Theoretical analyses revealed that electrons and negative and positive ions were produced under one negative power supply in the bipolar precharger simultaneously. Charged particles of opposite polarity, which escaped from the electric field with gas flow, deposited on the filter. Thus, the accumulative charge on fabric filter reduced due to charge neutralization. The influence of unipolar and bipolar prechargers on charge accumulation on the filter was experimental investigated. According to the maximum corona current, the optimized basic wire-tube electrode configuration was 120 mm in span of the tubes, 80 mm in wire-tube spacing, and 25 mm in tube diameter. The current on the filter, which was one order of magnitude lower than that in the precharger, was quadratic to the applied voltage on the precharger, and proportional to the gas velocity. Under gas velocities between 0.1 and 0.3 m s^{-1}, despite the corona current of the bipolar precharger was approximately 5% higher than that of the unipolar precharger, the accumulative charge on fabric filter surfaces was approximately 40%–50% lower than that of the filtration system with a unipolar precharger. The incorporation of a bipolar precharger into hybrid electrostatic filtration systems is a promising approach for reducing the risk of back corona and spark damage to the filter bag.

Keywords: Bipolar precharger, Charge accumulation, Charge neutralization, Back corona, Hybrid electrostatic Filtration systems

Received: January 25, 2022
Revised: April 7, 2022
Accepted: April 24, 2022

***Corresponding Authors:**
Pei Jia
ddjp1980@wit.edu.cn
Manqing Lin
14030102@wit.edu.cn

Publisher:
Taiwan Association for Aerosol Research
ISSN: 1680-8584 print
ISSN: 2071-1409 online

1 INTRODUCTION

Introducing electrostatic force into fabric filters is an effective, energy-efficient means of enhancing filtration performance. To comply with stringent emissions standards, hybrid electrostatic filtration systems designed for fine particles have been developed (Jaworek *et al.*, 2021; Ni *et al.*, 2018). The advantages of hybrid electrostatic filtration systems, such as their high efficiency in collecting fine particles and their relatively low energy consumption, have been demonstrated in experiments and in practice (Bekkara *et al.*, 2021; Kim *et al.*, 2018; Tian *et al.*, 2019; Xi *et al.*, 2021).

The effect of charged particles on filtration performance has been extensively investigated (Bruno *et al.*, 2020). Electric charge acts on filtration media through the following mechanism. Under the repulsive Coulomb force, charged particles are deposited on the surface of the filtration media rather than penetrating into the inner layers (Chang *et al.*, 2019; Givehchi *et al.*, 2015; Rodrigues *et al.*, 2017). The dust cake in an electrostatic field is more porous and fragile, which makes the deposited particles to be more easily dislodged from the filter surface by pulse jet cleaning. However, if the charged particles deposited on the filtration media cannot be removed in time, back corona or sparkover can occur due to the charge accumulation on the filter surface, causing spark damage to the filter bag (Choi *et al.*, 2018; Czech *et al.*, 2012; Plopeanu *et al.*, 2013).

Hybrid electrostatic filtration systems, such as compact hybrid particulate collectors and advanced hybrid particulate collectors, have been successfully applied in industry, and their

structures have undergone various improvements. However, the problems of back corona and spark damage have yet to be resolved. To prevent the occurrence of these phenomena, this study fabricated a wire-tube bipolar precharger to reduce the charge accumulation on the filter surface.

2 MATERIALS AND METHODS

2.1 Experimental Setup

The experimental platform (Fig. 1) comprised an aerosol generator, a precharger with a high voltage dc (HVDC) supply, a filter, a picoammeter (Model 6487, Tektronix, USA), and an exhaust fan.

The experimental chamber was made of a polymethyl methacrylate channel with a square cross section (950 × 950 mm^2) and a length of 1000 mm. Barbed wire is widely used as the corona electrode in industrial electrostatic precipitation (Yan *et al.*, 2019). Therefore, barbed wire and tubes were used in the precharger due to the lower pressure drop. The filter, made of conductive fibers 2 mm thick, was supported between two wire meshes.

The exhaust fan, installed at the end of the experimental platform, was employed to control the air flow rate by using a frequency converter. The gas velocity in the channel was measured with a hot wire anemometer (KA23, Kanomax, Japan). A self-constructed aerosol generator (50–5000 mg m^{-3}) was used to produce particles, which were injected into the channel through its inlet. The particle concentration was measured at the sample inlet of the channel by using a smoke and dust sampler (LY3012, Laoying, China). The voltage output and precharger current were read directly from the meters on the HVDC supply (BBG60, Jingcheng, China). The current on the filter was measured using a picoammeter.

2.2 Precharger Structure

To test the restraining effect of bipolar charging on charge accumulation on the filter, a unipolar precharger and a bipolar precharger were designed. When the electrodes were transverse to the gas flow, strong turbulent motion occurred in the precharger (Chang *et al.*, 2018). So, the electrodes in both unipolar precharger and bipolar precharger were placed transverse to the gas flow. Their geometries are presented in Fig. 2.

In the unipolar precharger, the barbed wires were placed equidistant from the parallel tubes. The tubes were grounded, and the barbed wires were set at negative HVDC. The negative ions and electrons were produced at the barbed wires and then moved toward the grounded tubes. In total, 6 barbed wires and 14 grounded tubes were used.

In the bipolar precharger, each parallel electrode configuration comprised both barbed wires and tubes. The negative electrodes were set under HVDC, and adjacent electrodes were grounded. The negative electrodes were placed equidistant from the grounded electrodes. A bipolar corona

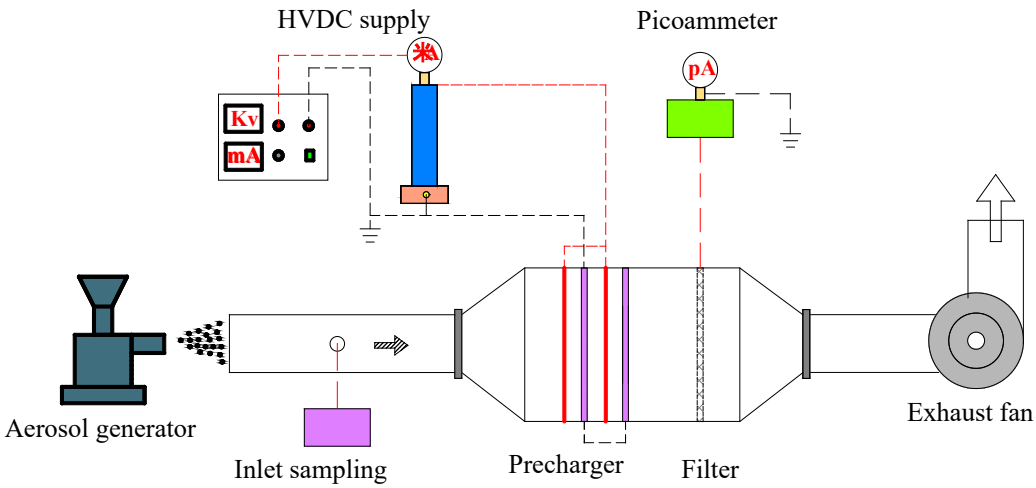

Fig. 1. Schematic of the experimental platform.

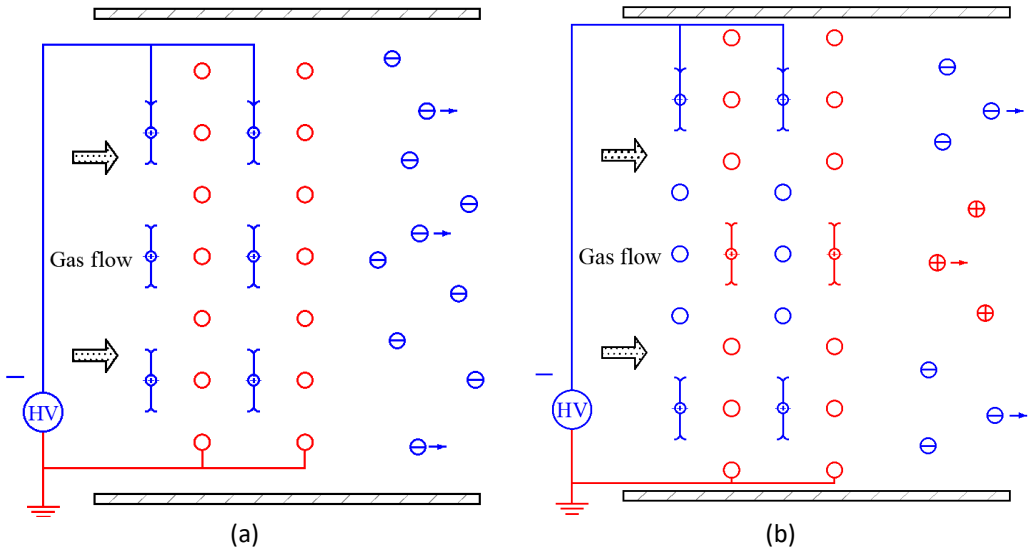

Fig. 2. Geometries of the (a) unipolar precharger and (b) bipolar precharger.

discharge can be achieved using only one HVDC supply (Xiang *et al.*, 2015). The negative ions and electrons were produced at the negative wires, and positive ions and electrons were produced at the grounded barbed wires. Six barbed wires and eighteen tubes were placed in the same area of the electric field. Thus, a bipolar precharger contained four more tubes than a unipolar precharger.

In both the unipolar and bipolar prechargers, one barbed wire and three tubes formed a basic wire-tube electrode (BWTE). Four negative BWTEs and two positive BWTEs were placed in the bipolar precharger; thus, the bipolar precharger had asymmetrical negative and positive discharges. In theory, the ratio of positive ions to negative ions is approximately 1:2, meaning that the charge at the outlet of the bipolar precharger should be one third that of the unipolar precharger because of charge neutralization.

Prechargers with different internal structures had different electric field distributions. In order to reveal the differences of electric field between unipolar precharger and bipolar precharger, commercial software COMSOL Multiphysics 5.5 was used for the solution of electric field based on the charge conservation equation coupling with Poisson's equation. Their electric field distributions are shown in Figs. 3 and 4.

In both the unipolar and bipolar prechargers, the corona discharge mainly occurred on the tips of the barbed wires (which were 120 mm apart) in the wire-tube electrodes (Guo *et al.*, 2014; Zheng *et al.*, 2018). Thus, a barbed wire can be represented by two wire electrodes 120 mm apart.

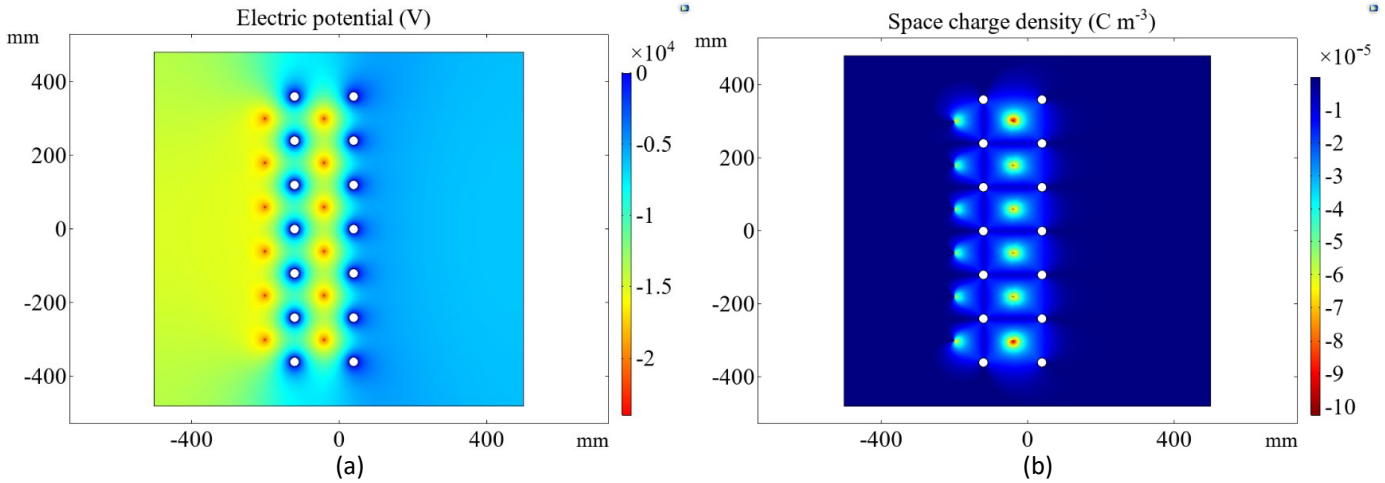

Fig. 3. Electric field distributions in the unipolar precharger: (a) electric potential and (b) space charge density.

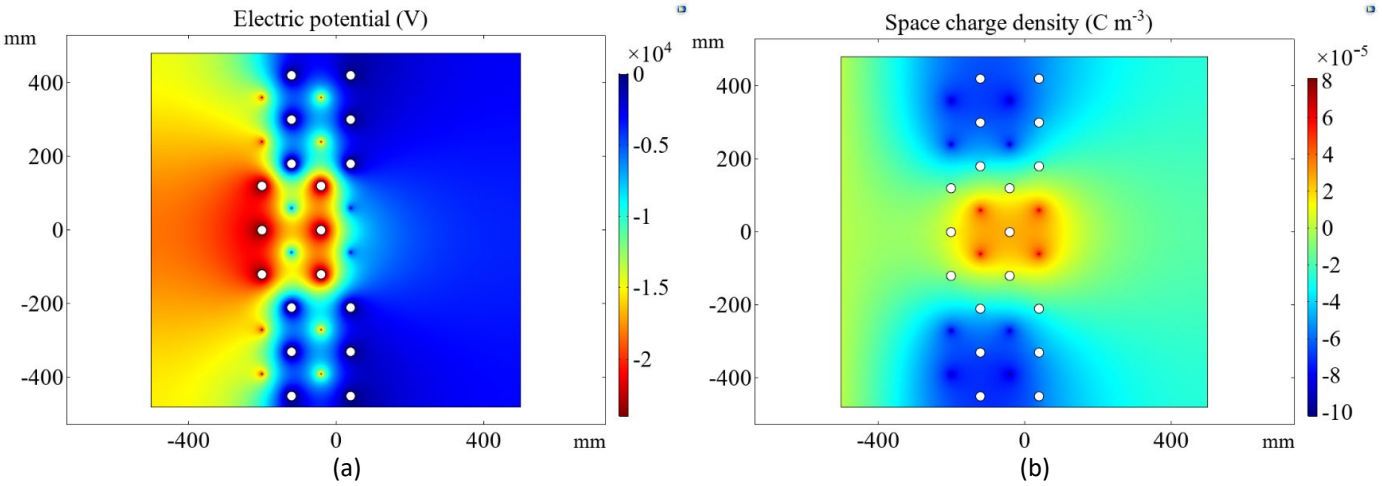

Fig. 4. Electric field distributions in the bipolar precharger: (a) electric potential and (b) space charge density.

In the unipolar precharger, the electric potential and space charge density decreased sharply from the negative wires to the grounded tubes; only negative ions and electrons were produced by a single source of negative HVDC.

In the bipolar precharger, the electric potential also decreased from the negative electrodes to the grounded electrodes. However, the negative space charge density declined abruptly from the negative wires to the grounded tubes, and the positive space charge density dropped sharply from the grounded wires to the negative tubes. Both electrons and negative and positive ions were produced by a single source of negative HVDC (Chang *et al.*, 2021).

2.3 Experimental Methods

Because the BWTE was the basic unit of the precharger, its configuration parameters determined the corona characteristics of the precharger (Chen *et al.*, 2021; Lee *et al.*, 2021). The configuration parameters affecting the corona current of the BWTE are *c*, *b* and *D*, where *c* is the span of the tubes, *b* is the space between the wires and the tubes, and *D* is the diameter of the tube electrode (Fig. 5). Because the distance between two tips of the barbed wire was 120 mm, *c* was set as 120 mm to obtain a symmetrical electric field. Therefore, *b* and *D* were the only geometric factors affecting the corona current of the BWTE.

In the experimental chamber, most of the ions and electrons were attached to suspended aerosols before moving toward the grounded electrodes under the Coulomb force. The remaining ions, which passed through the system via gas flow, were captured by the filter such that the charge accumulation on the filter was gradual. Directly measuring the charge accumulated on the filter

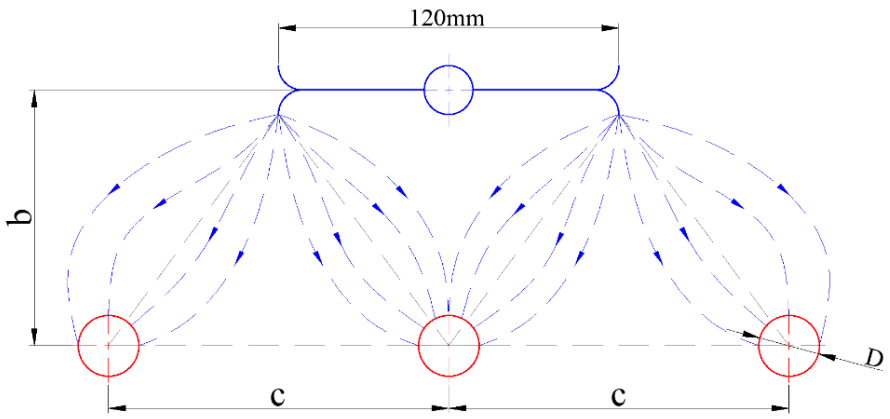

Fig. 5. Configuration parameters of the BWTEs.

was challenging, whereas the current on the grounded filter was easily determined (Kilic *et al.*, 2015; Yousefi *et al.*, 2018). Thus, to indirectly and qualitatively characterize the charge accumulation, this study measured the current produced by the charged particles on the filter using the picoammeter.

The experiments were conducted under laboratory conditions. The temperature was approximately 15 to 20°C, the relative humidity was 70%–80%, the concentration of dust at the inlet was approximately 700 mg m^{-3}, and the applied voltage was 25–30 kV. The gas velocity in the experimental chamber was 0.1–0.3 m s^{-1}, the same as the electric field velocity and the filtration velocity.

3 RESULTS AND DISCUSSION

3.1 Electrode Optimization of the Wire-tube Electrodes

3.1.1 Distance between the wires and the tubes

In the conventional electrostatic precipitator, the ratio of wire-wire spacing to wire-plate spacing is approximately 1–1.5. Because one barbed wire was represented as two wires 120 mm apart, the wire-tube distance was set to 60, 80, 100, 120, and 140 mm. To compare the discharging effect, the surface current density was defined as $i = Ib^{-1}c^{-1}$, where I is the corona current. The higher the current density is, the more favorable the discharge effect is under a given average electric field strength (Sundaram and Anandhraj, 2018). Fig. 6 presents the corona current density under various wire-tube spacings.

As presented in Fig. 6, the surface current density increased with the electric field strength. Given the higher electric fields at the wires, a wide wire-plate spacing was employed to enhance the collection efficiency. In the basic wire-tube electrode (BWTE), when the wire-tube spacing was 80 mm, the surface current density was maximized under an electric field strength between 2.5 and 3.0 kV cm^{-1}. From this result, 80 mm can be inferred to be the optimal wire-tube spacing.

3.1.2 Diameter of the tube electrode

Three stainless steel tubes (19, 25, and 32 mm in diameter) were selected as the dust collector electrodes. The voltage–current (V–I) characteristics of the BWTE were examined (Fig. 7).

As displayed in Fig. 7, the corona current increased with the applied voltage. Furthermore, it increased with the diameter of the tube because the area of dust collection expanded. However, the 25-mm and 32-mm tubes differed only slightly in V–I characteristics. To conserve materials and reduce the pressure drop, the 25-mm tube was determined to be the most suitable.

The optimal BWTE comprised one barbed wire and three tubes 25 mm in diameter, and the wire-tube spacing was 80 mm. The unipolar and bipolar prechargers consisted of multiple BWTEs in various permutations and combinations of.

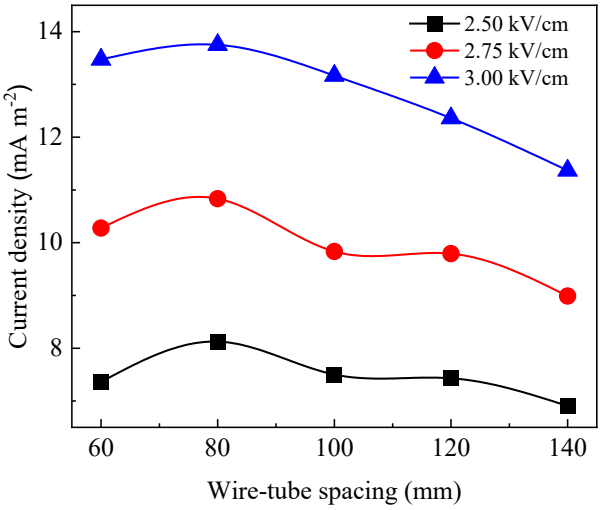

Fig. 6. Relationship between the current density and the wire-tube spacing (D = 25 mm).

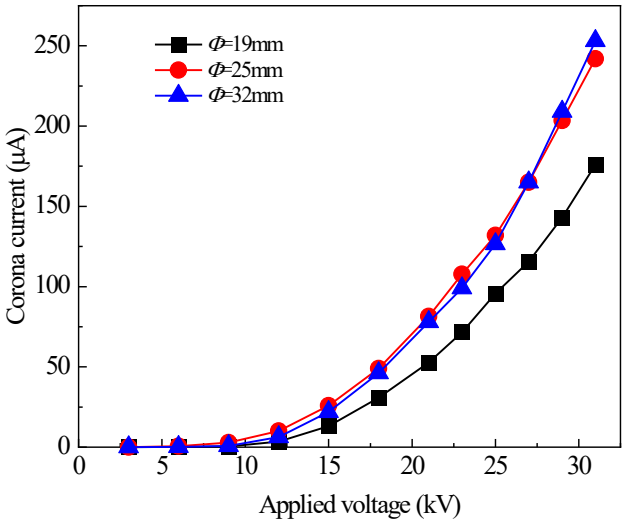

Fig. 7. *V–I* characteristics of the BWTE (*b* = 80 mm).

3.2 Corona Characteristics of the Prechargers

The *V–I* characteristics of the unipolar and bipolar prechargers when the electric field velocity was 0.17 m s^{-1} are presented in Fig. 8.

The relationship between the corona current and applied voltage was clearly quadratic. The corona current of the bipolar precharger was only 5% higher than that of the unipolar precharger at DC voltages between 25 and 30 kV. These results are attributable to the fact that more tubes were placed in the bipolar precharger than in the unipolar precharger in the same electric field space. However, due to the asymmetry of negative and positive BWTEs in the bipolar precharger, the corona current growth rate was not remarkable (Xiang *et al.*, 2015, Chang *et al.*, 2021). A higher corona current resulted in favorable particle charging in the bipolar precharger (Tu *et al.*, 2016). It was also found that the operating voltages of the bipolar precharger was slightly narrower than that of unipolar precharger, due to the lower breakdown potential of positive corona. Moreover, the corona starting voltage of the bipolar precharger was approximately 15 kV, similar to that of the unipolar precharger. In both the unipolar and bipolar prechargers, the *V–I* characteristics were not significantly affected by the electric field velocity.

So, the disadvantages of the bipolar precharger are higher initial investment cost, higher corona power consumption and narrower operating voltages.

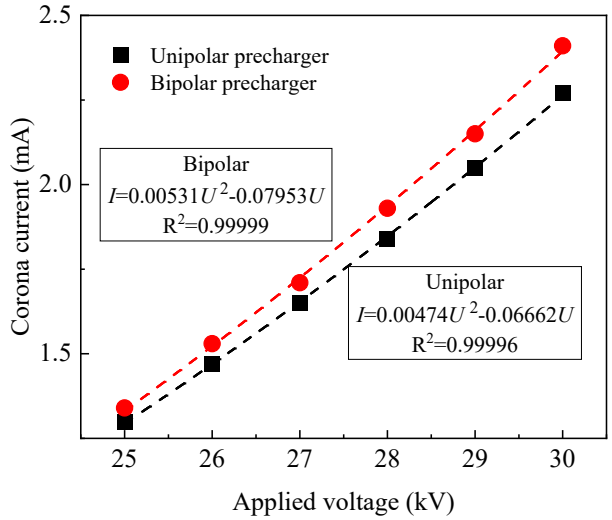

Fig. 8. *V–I* characteristics of the unipolar and bipolar prechargers.

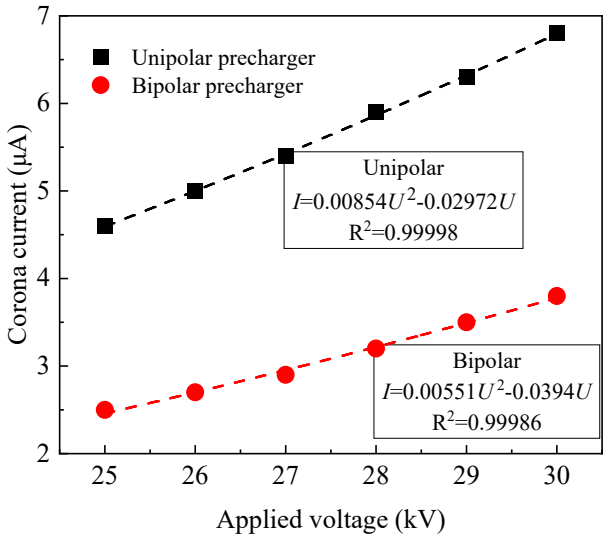

Fig. 9. Current produced by charged particles on the filter.

3.3 Charge Accumulation on the Filter

The currents produced by the charged particles on the filter when the filtration velocity was 0.17 m s^{-1} are displayed in Fig. 9.

The relationship between the current on the filter and the applied voltage on the precharger was clearly quadratic. The current produced by the bipolar charged particles was approximately 45% lower than that of the current produced by the unipolar charged particles. The charge reduction did not reach the theoretical value mentioned in Section 2.2 (approximately 2/3), possibly because the corona current of the bipolar precharger was higher than that of the unipolar precharger. Another explanation is that the current in the positive BWTE was lower than that in the negative BWTE (Chang *et al.*, 2018), which means that the bipolar precharger produced more negative ions and fewer positive ions relative to the theoretical value. The neutralization of positive and negative ions upstream of the filter reduced the charge accumulation on the filter; thus, the spark damage to the filter bag caused by charge accumulation was restrained.

The current on the filter was one order of magnitude lower than that in the precharger. Therefore, the charge escaping from the electric field negligibly affected the corona charge. However, it played a significant role on the collection efficiency and pressure drop in the filtration process (Jaworek *et al.*, 2019).

Gas flow was the force propelling the escape of charged particles from the electric field. Therefore, the current produced by charged particles under various gas velocities were measured in Fig. 10.

Furthermore, the current on the filter was approximately proportional to the gas velocity. A higher gas velocity facilitated the escape of charged particles from the electric field. Under gas velocities between 0.1 and 0.3 m s^{-1}, the current produced on the filter in the bipolar precharger was also approximately 40%–50% lower than that produced in the unipolar precharger. Therefore, the charge accumulation on the filter downstream of the bipolar precharger was reduced to a magnitude at which the back-corona discharge and spark damage to the filter bag was eliminated.

4 CONCLUSIONS

A wire-tube bipolar charging approach was applied to a hybrid electrostatic filtration system. The optimal wire-tube electrode configuration, corona characteristics of the prechargers, and charge accumulation on the filter were experimentally investigated under laboratory conditions. The conclusions are presented as follows.

1) The electrode configuration was optimized when the span of the tubes, wire-tube spacing, and tube diameter were 120, 80, and 25 mm, respectively.

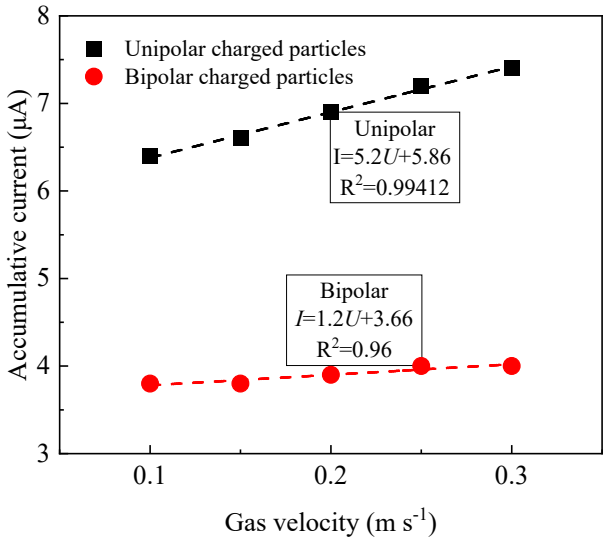

Fig. 10. Current produced by charged particles in different gas velocity.

2) In both the unipolar and bipolar prechargers, the relationship between the corona current and applied voltage was quadratic, and gas velocity exerted no significant effect on the *V–I* characteristics. The corona current of the bipolar precharger was approximately 5% higher than that of the unipolar precharger.
3) The relationship between the current on the filter and the applied voltage on the precharger was also quadratic, and the current on the filter was approximately proportional to the gas velocity. Under gas velocities between 0.1 and 0.3 m s^{-1}, the current produced on the filter in the bipolar precharger was approximately 40%–50% lower than that in the unipolar precharger.

ACKNOWLEDGMENT

This work was supported by 2021 Hubei Provincial Department of Education Scientific Research Plan Guiding Project (No. B2021082), and the National Natural Science Foundation of China (No. 52174085). This manuscript was edited by Wallace Academic Editing.

REFERENCES

Bekkara, F., Benmimoun Y., Kheiter A., Chelih A., Tilmatine A. (2021). Electrostatic charge decay and filtration performance of nonwoven filters in the vicinity of grounded metal grids. J. Electrost. 110, 103554. https://doi.org/10.1016/j.elstat.2021.103554

Bruno, J., Rafael, S., Vádila, G., Mônica, L. (2020). Hybrid air filters: A review of the main equipment configurations and results. Process Saf. Environ. Prot. 144, 193–207. https://doi.org/10.1016/j.psep.2020.07.025

Chang, Y., Jia, P., Shi, L., Xiang, X. (2018). Corona discharging and particle collection of bipolar transverse plate ESP. J. Electrost. 96, 104–110. https://doi.org/10.1016/j.elstat.2018.10.004

Chang, Y., Jia, P., Xiang, X., Shi, L., Jiang, X. (2019). Investigation of the performance of filtration-charged particles in a reversed electric field. Aerosol Air Qual. Res. 19, 2879–2887. https://doi.org/10.4209/aaqr.2019.06.0283

Chang, Y., Shi, L., Jia, P. (2021). Bipolar precharger for hybrid electrostatic filtration systems. Aerosol Air Qual. Res. 21, 210199. https://doi.org/10.4209/aaqr.210199

Chen, B., Guo, Y., Li, H., Zhou, W., Liu, B. (2021). Discharge characteristic of barbed electrodes in electrostatic precipitator. J. Electrost. 109, 103528. https://doi.org/10.1016/j.elstat.2020.103528

Choi, D., An, E., Jung, S., Song, D., Oh, Y., Lee, H., Lee, H. (2018). Al-coated conductive fiber filters for high-efficiency electrostatic filtration: Effects of electrical and fiber structural properties. Sci. Rep. 8, 5747. https://doi.org/10.1038/s41598-018-23960-9

Czech, T., Sobczyk, A., Jaworek, A., Krupa, A. (2012). Corona and back discharges in flue-gas simulating mixture. J. Electrost. 70, 269–284. https://doi.org/10.1016/j.elstat.2012.03.005

Givehchi, R., Li, Q., Tan, Z. (2015). The effect of electrostatic forces on filtration efficiency of granular filters. Powder Technol. 277, 135–140. https://doi.org/10.1016/j.powtec.2015.01.074

Guo, B., Guo, J., Yu, A. (2014). Simulation of the electric field in wire-plate type electrostatic precipitators. J. Electrost. 72, 301–310. https://doi.org/10.1016/j.elstat.2014.05.005

Jaworek, A., Sobczyk, A.T., Krupa, A., Marchewicz, A., Czech, T., Śliwiński, L. (2019). Hybrid electrostatic filtration systems for fly ash particles emission control. A review. Sep. Purif. Technol. 213, 283–302. https://doi.org/10.1016/j.seppur.2018.12.011

Jaworek, A., Sobczyk, A., Krupa, A., Marchewicz, A., Czech, T., Śliwiński, L., Boryczko, G. (2021). Hybrid electrostatic filtration system for fly ash particles emission control. J. Electrost. 114, 103628. https://doi.org/10.1016/j.elstat.2021.103628

Kilic, A., Shim, E., Pourdeyhimi, B. (2015). Measuring electrostatic properties of fibrous materials: A review and a modified surface potential decay technique. J. Electrost. 74, 21–26. https://doi.org/10.1016/j.elstat.2014.12.007

Kim, M., Lim, G., Kim Y., Han, B., Woo, C., Kim, H. (2018). A novel electrostatic precipitator-type small air purifier with a carbon fiber ionizer and an activated carbon fiber filter. Aerosol Sci. Technol. 117, 63–73. https://doi.org/10.1016/j.jaerosci.2017.12.014

Lee, G., Hwang, Y., Cheon, T., Kim, H., Han, B., Yook, S. (2021). Optimization of pipe-and-spike discharge electrode shape for improving electrostatic precipitator collection efficiency. Powder Technol. 379, 241–250. https://doi.org/10.1016/j.powtec.2020.10.044

Ni, Z., Luo, K., Gao, Y., Gao, X., Fan, J., Cen, K. (2018). Potential air quality improvements from ultralow emissions at coal-fired power plants in China. Aerosol Air Qual. Res. 18, 1944–1951. https://doi.org/10.4209/aaqr.2018.02.0070

Plopeanu, M., Dascalescu, L., Neagoe, B., Bendaoud, A., Notingher, P. (2013). Characterization of two electrode systems for corona-charging of non-woven filter media. J. Electrost. 71, 517–523. https://doi.org/10.1016/j.elstat.2012.12.002

Rodrigues, M., Barrozo, M., Gonçalves, J., Coury, J. (2017). Effect of particle electrostatic charge on aerosol filtration by a fibrous filter. Powder Technol. 313, 323–331. https://doi.org/10.1016/j.powtec.2017.03.033

Sundaram, K., Anandhraj, P. (2018). Design and analysis of electric potential and space charge density in a portable electrostatic precipitator. Results Phys. 11, 1054–1055. https://doi.org/10.1016/j.rinp.2018.10.060

Tian, E., Mo, J., Li, X. (2018). Electrostatically assisted metal foam coarse filter with small pressure drop for efficient removal of fine particles: Effect of filter medium. Build. Environ. 144, 419–426. https://doi.org/10.1016/j.buildenv.2018.08.026

Tu, G., Song, Q., Yao, Q. (2016). Relationship between particle charge and electrostatic enhancement of filter performance. Powder Technol. 301, 665–673. https://doi.org/10.1016/j.powtec.2016.06.044

Xi, J., Gu, Z., Cai, J., Zhang, J., Wang, H., Wang, S. (2021). Filtration of dust in an electrostatically enhanced granular bed filter for high temperature gas cleanup. Powder Technol. 368, 105–111. https://doi.org/10.1016/j.powtec.2020.03.070

Xiang, X., Chang, Y., Nie, Y. (2015) Investigation of the performance of bipolar transverse plate ESP in the sintering flue control. J. Electrost. 76, 18–23. https://doi.org/10.1016/j.elstat.2015.04.003

Yan, D., Zhang, Z., Gong, H., Ya, Y. (2019). Effect of barbed tubular electrode corona discharge EHD flow on submicron particle collection in a wide-type ESP. J. Electrost. 109, 103545. https://doi.org/10.1016/j.elstat.2020.103545

Yousefi, S., Venkateshan, D., Tang, C., Tafreshi, H., Pourdeyhimi, B. (2018). Effects of electrospinning conditions on microstructural properties of polystyrene fibrous materials. J. Appl. Phys. 124, 235307. https://doi.org/10.1063/1.5049128

Zheng, C., Wang, Y., Zhang, X., Yang, Z., Liu, A., Guo, Y., Zhang, Y., Wang, Y., Gao, X. (2018). Current density distribution and optimization of the collection electrodes of a honeycomb wet electrostatic precipitator. RSC Adv. 8, 30701–30711. https://doi.org/10.1039/C8RA04765K